Journal of Cellular Physiology

A peptide that blocks the interaction of NF-κB p65 subunit with Smad4 enhances BMP2-induced osteogenesis.

Journal:	*Journal of Cellular Physiology*
Manuscript ID	JCP-17-1095.R1
Wiley - Manuscript type:	Original Research Article
Date Submitted by the Author:	23-Feb-2018
Complete List of Authors:	Urata, Mariko ; Kyushu Shika Daigaku, Oral Function Kokabu, Shoichiro; Kyushu Shika Daigaku, Health Promotion Matsubara, Takuma; Kyushu Shika Daigaku, Health Promotion Sugiyama, Goro; Kyushu University, Oral and Maxillofacial Surgery Nakatomi, Chihiro; Kyushu Shika Daigaku, Health Promotion Takeuchi, Hiroshi; Kyushu Shika Daigaku, Health Promotion Hirata-Tsuchiya, Shizu; Hiroshima University, Biological Endodontics Aoki, Kazuhiro; Tokyo medical and Dental University, Hard tissue engineering Tamura, Yukihiko; Tokyo Medical and Dental University Moriyama, Yasuko; Kyushu University, Oral Rehabilitation Ayukawa, Yasunori; Kyushu University, Faculty of Dental Science, , Implant & Rehabilitative Dentistry Matsuda, Miho; Kyushu University, Molecular and Cellular Biochemistry Zhang, Min; Kyushu Shika Daigaku, Health Promotion Koyano, Kiyoshi; Kyushu University, Faculty of Dental Science, , Implant & Rehabilitative Dentistry Kitamura, Chiaki; Kyushu Shika Daigaku, Oral Function Jimi, Ejiro; Kyushu Daigaku, OBT Reserch Center
Key Words:	BMP, osteoblasts, NF-κB

MS#17-1095R1

A peptide that blocks the interaction of NF-κB p65 subunit with Smad4 enhances BMP2-induced osteogenesis

Mariko Urata[1,2], Shoichiro Kokabu[1], Takuma Matsubara[1], Goro Sugiyama[3], Chihiro Nakatomi[1], Hiroshi Takeuchi[1], Shizu Hirata-Tsuchiya[4], Kazuhiro Aoki[5], Yukihiko Tamura[6], Yasuko Moriyama[7], Yasunori Ayukawa[7], Miho Matsuda[8], Min Zhang[1], Kiyoshi Koyano[7], Chiaki Kitamura[2], Eijiro Jimi[1,8,9]

[1] Department of Health Promotion, [2] Department of Oral Function, Kyushu Dental University, Fukuoka, 803-8580, Japan;

[3] Section of Oral and Maxillofacial Surgery, Division of Maxillofacial Diagnostic and Surgical Sciences, Graduate School of Dental Science, Kyushu University, Fukuoka, 812-8582, Japan;

[4] Department of Biological Endodontics, Integrated Health Sciences, Institute of Biomedical and Health Sciences, Hiroshima University, Hiroshima, 734-8553, Japan;

[5] Department of Functional Dentistry, [6] Department of Bio-Matrix, Graduate School of Medical and Dental Sciences, Tokyo Medical and Dental University, Tokyo, 113-8510, Japan;

[7] Section of Implant and Rehabilitative Dentistry, Division of Oral Rehabilitation, [8] Laboratory of Molecular and Cellular Biochemistry, Faculty of Dental Science, Kyushu University, Fukuoka, 812-8582, Japan;

[9] Oral Health/Brain Health/Total Health Research Center, Faculty of Dental Science, Kyushu University, Fukuoka, 812-8582, Japan

Corresponding author

Eijiro Jimi

Oral Health/Brain Health/Total Health Research Center, Faculty of Dental Science, Kyushu University,

[redacted]

Running title: Effects of SBD peptide on BMP-induced osteogenesis

Key words: BMP, osteoblasts, NF-κB

Total number of figures: 6, supplemental figures: 2

This work was supported by grants-in-aid from Kyushu Dental University Internal Grants (to E.J.) and from the Ministry of Education, Culture, Sports, Science and Technology of Japan (JP16K11456 to M.Z., JP26293406 to C.K., and JP17K11706 to S.H.-T.).

Abstract

Bone morphogenetic protein (BMP) potentiates bone formation through the Smad signaling pathway *in vitro* and *in vivo*. The transcription factor nuclear factor κB (NF-κB) suppresses BMP-induced osteoblast differentiation. Recently, we identified that the transactivation (TA) 2 domain of p65, a main subunit of NF-κB, interacts with the mad homology (MH) 1 domain of Smad4 to inhibit BMP signaling. Therefore, we further attempted to identify the interacting regions of these two molecules at the amino acid level. We identified a region that we term the Smad4-binding domain (SBD), an amino-terminal region of TA2 that associates with the MH1 domain of Smad4. Cell-permeable SBD peptide blocked the association of p65 with Smad4 and enhanced BMP2-induced osteoblast differentiation and mineralization without affecting the phosphorylation of Smad1/5 or the activation of NF-κB signaling. SBD peptide enhanced the binding of the BMP2-inudced phosphorylated Smad1/5 on the promoter region of inhibitor of DNA binding 1 (Id-1) compared with control peptide. Although SBD peptide did not affect BMP2-induced chondrogenesis during ectopic bone formation, the peptide enhanced BMP2-induced ectopic bone formation in subcortical bone. Thus, the SBD peptide is useful for enabling BMP2-induced bone regeneration without inhibiting NF-κB activity (191 words).

Introduction

Bone remodeling consists of bone resorption by osteoclasts and bone formation by osteoblasts and is important for maintenance of bone mass and calcium homeostasis. Bone resorption and bone formation are tightly coupled, but if the balance between these two events is lost, bone mass increases or decreases (Kobayashi Y et al., 2016; Zhao B. 2017). Osteoporosis, arthritis and periodontal diseases are caused by enhancement of bone resorption, and the anti-bone-resorption drugs that are currently in common clinical use are bisphosphonates, selective estrogen modulator (SERM) and anti-RANKL monoclonal antibody (denosumab) (Chen JS and Sambrook PN. 2011). The inhibition of bone resorption alone is not sufficient to regenerate new bone to repair bone loss. Thus, developing new approaches that may stimulate osteoblastogenesis is desirable.

Osteoblasts—bone-forming cells—differentiate from mesenchymal stem cells. Osteoblast differentiation is regulated by various factors including hormones and local factors, which induce their maturation and mineralization (Kobayashi Y et al., 2016; Zhao B. 2017). Among those factors, bone morphogenetic protein (BMP) is one of the most potent inducers of osteoblastic bone formation. BMP signaling is strictly regulated at numerous steps, from ligand availability to the nuclear factors that regulate their transcriptional response. The binding of BMP to BMP receptors phosphorylates Smad1/5 in the cytoplasm. The signal is then transduced via the complex formed by Smad1/5 and Smad4 and is subsequently translocated into the nucleus to regulate BMP-specific target gene expression. The Smad proteins contain 2 conserved globular domains called the mad homology (MH) 1 and MH2 domains. The MH1 domain of Smad4 directly interacts with DNA, and the MH2 domain binds to the phosphorylated C-tail of activated Smad1/5, suggesting that these domains of Smad4 are important for BMP signaling (Jimi E. 2015; Katagiri T and Watabe T. 2016).

Aside from the classical Smad pathway, BMPs also activate Smad-independent signaling pathways, such as mitogen-activated protein kinase (MAPK), phosphoinositide 3-kinase (PI3K) and nuclear factor κB (NF-κB) etc (Jimi E. 2015). Among them, recent findings revealed the importance of NF-κB in osteoblast differentiation and bone formation. The inhibition of NF-κB in mature mouse osteoblasts by expressing a dominant negative form of IκB kinase (IKK) β increased bone volume and bone mineral density (BMD) by increasing osteoblast activity (Chang J et al., 2009; Krum SA et al., 2010). The selective inhibition of NF-κB prevented bone loss in ovariectomized mice (Alles M et al., 2010). We also reported that the selective inhibition of NF-κB enhanced BMP-induced osteoblast differentiation and ectopic bone formation (Yamazaki M et al., 2009; Hirata-Tsuchiya S et al., 2014). However, mice lacking p65, a main subunit of NF-κB, die as embryos (Beg AA et al., 1995), indicating that the inhibition of the NF-κB pathway leads to severe side effects.

Thus, we examined the molecular mechanism by which NF-κB suppresses BMP-induced osteoblast differentiation and bone formation. We found that NF-κB suppressed BMP-induced osteogenesis by inhibiting the DNA binding of the Smad1/5-Smad4 complex through the interaction of p65 with Smad4. Furthermore, we identified that transactivation (TA) 2 domain of p65 interacted with the MH1 domain of Smad4 (Hirata-Tsuchiya S et al., 2014).

In this study, we further narrowed the range of possible interacting regions of these two domains and generated a cell-permeable peptide—termed Smad4-binding domain (SBD) peptide—that disrupts the interaction of p65 with Smad4. Then, we examined the effects of SBD peptide on BMP2-induced osteoblast differentiation and ectopic bone formation.

Materials and Methods

The experimental procedures were approved by the Animal Care and Use Committee

of Kyushu Dental University (approval number 16-036).

Reagents. Purified recombinant human BMP2 was purchased from R&D Systems (Minneapolis, MN). Anti-phosphorylated Smad1/5 (no. 9516), anti-Smad1 (no. 9743), anti-Smad4 (no. 38454) and anti-phosphorylated p65 (no. 3031) antibodies were obtained from Cell Signaling Technology, Inc (Beverly, MA). Anti-IκBα (sc-371) antibodies were obtained from Santa Cruz Biotechnology (Santa Cruz, CA). Anti-p65 (SA171) antibodies were obtained from Biomol (Plymouth Meeting PA). Anti-FLAG M5 and anti-β-actin (AC-15) antibodies were purchased from Sigma-Aldrich (St. Louis, MO). Anti-Myc, anti-GST, and anti-His antibodies were purchased from Medical and Biological Laboratories (Nagoya, Japan).

Recombinant protein expression in bacteria and GST pull-down assay. For glutathione S-transferase (GST) fusion proteins, different portions of the TA2 domain of p65 and a His-tagged MH1 domain of Smad4 were cloned into pGEX vectors (GE Healthcare Life Sciences, Buckinghamshire, UK) and pET-His30 vector (Takara Bio, Shiga, Japan), respectively. GST- or His-tagged proteins were prepared using the same standard procedure with the same schedule to grow bacteria and induce the expression of the recombinant proteins described previously (Sugiyama G. et al., 2011). In GST pull-down assays, equal amounts of GST fusion proteins were immobilized on glutathione-agarose beads and incubated at 4 °C for 30 min with His-tagged MH1 of Smad4. At the end of the incubation, the beads were washed with the reaction buffer (20 mM HEPES-NaOH (pH 7.4), 150 mM NaCl, 1 mM EDTA, 1% Triton X-100) three times, boiled in 50 μL of sample buffer for 5 min, and subjected to SDS−PAGE followed by Western blotting. The bound MH1 domain of Smad4 was detected with anti-His antibody.

Peptide synthesis. Peptide with the following sequences were synthesized by Eurofingenomics (Tokyo, Japan): wild-type (WT) SBD peptide, NH_2-RRRRRRRRR-GGG-QAGEGTLSEALLHLQF-COOH; scramble (Scr) peptide, NH_2-RRRRRRRRR-GGG-LGSLAHQLAQGFTELE-COOH; WT SBD peptide for pull-down assay (without a poly-arginine; WT-polyR), NH_2-GGG-QAGEGTLSEALLHLQF-COOH; Scr peptide for pull-down assay (without a poly-arginine; Scr-polyR), NH_2-GGG-LGSLAHQLAQGFTELE-COOH.

Cell culture. MC3T3-E1 mouse osteoblast cells, obtained from RIKEN Cell Bank (Tsukuba, Japan), were maintained in minimal essential medium (MEM) α containing 10% fetal bovine serum (FBS), 100 U/ml penicillin, and 100 μg/ml streptomycin. Primary osteoblasts (POB) were prepared from the calvariae of 1-day-old C57BL/6 mice by digestion with 0.1% collagenase (Wako, Osaka, Japan) and 0.2% dispase (Godo Shusei, Tokyo, Japan). POB were maintained in MEM α containing 10% FBS and antibiotics. COS7 cells, an African green monkey cell line producing Simian Virus 40 (SV40) T antigen, were obtained from JCRB Cell Bank (Osaka, Japan) and maintained in Dulbecco's modified Eagle's medium (DMEM) containing 10% FBS and antibiotics. p65-deficient (p65-/-) mouse embryonic fibroblasts (MEFs) prepared as described previously, were maintained in DMEM ontaining 10% FBS and antibiotics (Hirata-Tsuchiya S et al., 2014).

Detection of alkaline phosphatase (ALP) activity and staining. MC3T3-E1 cells or POBs were seeded the day before treatment at a density of 1.0×10^4 cells per well in 96-well plates with MEM α containing 5% FBS. p65-/- MEFs were seeded the day before treatment at a density of 5.0×10^3 cells per well in 96-well plates with DMEM α containing 5% FBS. The cells were treated with BMP2 (100 ng/ml) with or without several concentrations of WT SBD or Scr peptide for 72 hr. In some experiments,

MC3T3-E1 cells were transfected with either FLAG-tagged TA2 or FLAG-tagged TA2 (444-521) using Lipofectamine 2000 (Invitrogen, Carlsbad, CA) and then treated with BMP2 (100 ng/ml) for 72 hr. After treatment, the cells were fixed with an acetone/ethanol mixture (50:50, v/v) and then incubated with a substrate solution (0.1 M diethanolamine, 1 mM $MgCl_2$, and 10 mg/ml p-nitrophenyl phosphate). Reactions were stopped by adding 5 M NaOH, and the absorbance was measured at 405 nm using a microplate reader (Bio-Rad Laboratories, Inc., Hercules, CA). Histochemical measurements of ALP enzyme activity were performed as described previously (Katagiri T et al., 1994).

Real-time polymerase chain reaction (PCR) analysis. Real-time PCR was performed using SYBR Green Master Mix and a 7300 real-time PCR system (Applied Biosystems, Foster City, CA) according to the manufacture's instructions. The samples were matched to a standard curve generated by amplifying serially diluted products as an internal control. The primer sequences have been described previously (Hirata S et al., 2010).

Alizarin red S staining. Primary osteobalsts were seeded at a density of 2.0×10^4 cells per well in 48-well plates with MEM α containing 5% FBS, 50 μg/ml ascorbic acid, 10 nM dexamethasone, and 5 mM β-glycerophosphate. The cells were treated with BMP2 (100 ng/ml) with or without several concentrations of WT SBD or Scr peptide for 14 days. After treatment, the cells were fixed with 10% (v/v) formalin in PBS for 30 min and washed three times using deionized water. The cells were stained with 1% alizarin red S solution for 30 min at room temperature. Alizarin red dye was extracted with 10% formic acid, and the absorbance at 405 nm was determined with a microplate reader.

Cell proliferation assay. Proliferation of MC3T3-E1 cells was measured using the Cell Counting Kit-8 (Dojindo, Kumamoto, Japan) according to the manufacturer's instructions.

Western blot analysis and immunoprecipitation. Cells were lysed in TNT buffer (20 mM Tris-HCl, pH 7.5; 200 mM NaCl, 1% Triton X-100, and 1 mM dithiothreitol) containing protease inhibitors and phosphatase inhibitors (Roche, Basel, Switzerland). The protein content was measured with Pierce reagent following the manufacturer's protocol. The lysates were resolved by 10% SDS-PAGE, transferred to Immobilon-P membranes (Millipore Corp., Billerica, MA), and immunoblotted with individual antibodies. Then, the membranes were washed and incubated with horseradish peroxidase-conjugated secondary antibodies (Santa Cruz Biotechnology). The immunoreactive proteins were visualized using ECL (Amersham Pharmacia Biotech, Piscataway, NJ) and were analyzed with a Luminescent Image Analyzer (Fujifilm, Tokyo, Japan). For the co-precipitation experiments, whole-cell extracts were incubated for 6 hours at 4°C with anti-FLAG or anti-Myc antibodies coupled to A/G Sepharose beads. The immune complex was extensively washed with TNT buffer, and the samples were boiled and analyzed by immunoblotting.

Chromatin immunoprecipitation (ChIP) Assays. ChIP was performed with a ChIP assay kit (Cell Signaling, #9005) according to the manufacturer's instructions, using antibodies against phosphorylated Smad1/5 antibodies as previously described (Hirata-Tsuchiya S et al., 2014).

Ectopic bone formation assay. The bone formation effects induced by BMP2 *in vivo* were examined using an ectopic bone formation assay in the presence or absence of WT SBD peptide in mice. BMP2 (1 μg) and WT SBD peptide (100 or 200 μg) were blotted

onto a collagen sponge disk (4-mm diameter, 1-mm thickness) made from commercially available bovine collagen sheets (Helistat; Integra Neurosciences), freeze-dried, and maintained at -20°C until they were implanted into the mice (Zhao B et al., 2006). All procedures were performed under sterile conditions. The mice were anesthetized by isoflurane inhalation, and collagen pellets were surgically implanted into the dorsal muscle pouches (3 pellets/animal) of the mice (8 weeks old). Days 7 and 21 after surgery, the mice were euthanized, and the implants were harvested and processed for histological analysis. All of the harvested samples were fixed in PBS-buffered glutaraldehyde (0.25%)-formalin (4%) fixative (pH 7.4) for 2 days at 4°C and washed with PBS for further studies. To distinguish cartilage matrix, Alcian blue stains proteoglycans of cartilaginous matrix and connective tissue turquoise blue and nuclei of cells are stained pale violet by hematoxylin in sections of each group. To quantify cartilage formation, the width of the column structure of cartilage and the area of cartilage was divided by the area of the whole pellet were measured. The BMD of the ectopic bone was measured using dual-energy X-ray absorptiometry (DCS-600R; Aloka, Tokyo, Japan). Three-dimensional reconstruction images of the ectopic bone were obtained by micro-computed tomography (μCT) (ScanXmate-E090; Comscan, Yokohama, Japan) as described previously. Sections of ectopic bone from each group were stained with Hematoxylin-Eosin (HE) and tartrate-resistant acid phosphatase (TRAP). The sections were examined using light microscopy.

Data analysis. Comparisons were made using an unpaired Student's t-test. The data are expressed as the means ± SD; values of $P < 0.05$ were considered significant.

Results

Interaction between the NH_2-terminal region of the TA2 domain of p65 and the MH1 domain of Smad4.

We previously found using co-immunoprecipitation that the TA2 domain of p65 interacted with the MH1 domain of Smad4 (Hirata-Tsuchiya S et al., 2014). Thus, to examine whether the TA2 domain of p65 directly interacts with the MH1 domain of Smad4, we generated TA2 fused with GST (GST-TA2) and His-tagged MH1 (His-MH1) (Figure 1a, left panel). We then mixed these proteins, and after a short incubation period, the GST proteins were precipitated by binding to glutathione-agarose beads and were then washed extensively. GST-TA2 but not GST alone bound to His-MH1, suggesting that the TA2 domain of p65 directly bound to the MH1 domain of Smad4 (Figure 1a, right panel).

To identify the interacting region of TA2, we generated several truncated mutants of TA2 fused with GST (Figure 1b). All three NH_2-terminal fragments (428-521, 428-508, 428-443) but not 444-521 interacted with His-MH1, indicating that the interaction domain lies between residues 428 and 443 (Figure 1c). Therefore, we have named this sequence the Smad4-binding domain (SBD).

Inhibition of p65-Smad4 interaction by cell-permeable peptide spanning the p65 SBD.

We designed cell-permeable peptide spanning the p65 SBD and determined their ability to disrupt p65-Smad4 interaction. The WT SBD peptide consisted of the region from Q428 to F443 of p65 fused with poly-arginine, which mediates membrane translocation. The peptide targeted the same amino acids as WT SBD peptide, and scrambled sequences (Scr) were used as control peptide. Only WT SBD peptide inhibited *in vitro* interaction between GST-TA2 and His-MH1 (Figure 2a). Furthermore, WT SBD, but not Scr peptide inhibited the interaction of FLAG-p65 with Myc-Smad4, as measured by co-immunoprecipitation (Figure 2b).

SBD peptide enhanced BMP2-induced osteoblast differentiation.

We next examined the effects of SBD peptide on BMP2-induced osteoblast differentiation using the mouse osteoblastic cell line MC3T3-E1. WT SBD peptide did not induce ALP activity in the absence of BMP2 but strongly promoted ALP activity in a dose-dependent manner in the presence of BMP2 (Figure 3a). The number of cells that became ALP positive in response to BMP was also increased in the presence of WT SBD peptide, but not Scr peptide (Figure 3b). The WT SBD peptide without a poly-arginine failed to enhance BMP2-induced ALP activity, suggesting that WT SBD peptide stimulated the activity in cells (Figure 3a). Neither SBD peptide nor Scr peptide affected the proliferation of MC3T3-E1 cells in the presence or absence of BMP2 (Figure S1). The WT SBD peptide, but not the Scr peptide, enhanced BMP2-induced ALP activity in mouse primary osteoblasts (Figure S2). Furthermore, WT SBD peptide did not affect BMP2-induced ALP activity in p65-/-MEFs (Figure 3c). The BMP2-induced ALP activity was enhanced in the presence of FLAG-tagged TA2, but not FLAG-tagged TA2 (444-521), suggesting that WT SBD peptide specifically enhanced BMP2-induced ALP activity (Figure 3d). BMP2-induced expressions of type I collagen, osteonectin and osteocalcin in association with osteoblast differentiation were also augmented in the presence of WT SBD peptides (Figure 3e). Furthermore, WT SBD peptide stimulated BMP2-induced mineralization compared with Scr peptides (Figure 3f).

SBD peptide enhanced BMP-induced transcriptional activity of Smad1/5 without affecting NF-κB activity.

We next examined the effects of SBD peptide on the phosphorylation of Smad1/5, an initial key step in the BMP signaling pathway. Neither WT SBD nor Scr peptide affected BMP2-induced phosphorylation of Smad1/5, expression levels of Smad1 and Smad4 (Figure 4a). However, as previously reported (Hirata-Tsuchiya S et al., 2014), phosphorylated Smad1/5 bound to the Id1 promoter longer in the presence of WT SBD

peptide than in the absence of WT SBD peptide or in the presence of Scr peptide (Figure 4b). Consistent with Fig. 4b, WT SBD but not Scr peptide enhanced the expression levels of BMP target genes, such as Id1 and osterix (OSX) (Figures 4c and 4d).

Several lines of evidence have shown that inhibition of NF-κB by specific inhibitors enhances BMP-induced osteogenesis (Chang J et al., 2009; Yamazaki M et al., 2009; Alles M et al., 2010; Hirata-Tsuchiya S et al., 2014). However, long-term treatment with NF-κB inhibitors might induce unexpected side effects because mice deficient in p65 die as embryos (Beg AA et al., 1995). Thus, we subsequently examined the effects of SBD peptide on TNFα-induced NF-κB activity. Neither the degradation of IκBα nor the phosphorylation of p65 was affected by treatment with TNFα in the presence or absence of either SBD peptide (Figure 4e). Neither WT SBD nor Scr peptide affected TNFα-induced expression of IL-6, a typical target gene of NF-κB (Ghosh S and Dass JF. 2016) (Figure 4f). These results suggest that WT SBD but not Scr peptide enhance BMP-induced transcriptional activity of Smad1/5 and that they do so without affecting Smad phosphorylation or TNFα-induced NF-κB activity.

SBD peptide did not significantly affect BMP2-induced chondrogenesis during ectopic bone formation.

We examined the effects of WT SBD peptide on BMP2-induced chondrogenesis during ectopic bone formation. Collagen sponges soaked with 1 μg of BMP2 with or without WT SBD peptide were implanted in the dorsal fascia of normal mice. After 1 week, the size of pellet was comparable in the presence and absence of WT SBD peptide (data not shown). The histological analysis showed that irregularly arranged collagen fiber-like structures and chondroid matrix containing mature and hypertrophic chondrocytes at the pellet rim in the presence and absence of WT SBD peptide (Figures 5a). The width of the column structure of cartilage in the presence of 100 μg of WT

SBD peptide was longer than that of BMP2 alone or in the presence of 200 μg of WT SBD peptide (Figure 5b). The area of cartilage divided by the area of the whole pellet in the presence of 100 μg of WT SBD peptide was slightly larger than that of either BMP2 alone or in the presence of 200 μg of WT SBD peptide without any significance (Figure 5b). These results suggest that SBD peptide did not significantly affect BMP2-induced chondrogenesis.

SBD peptide stimulated BMP2-induced ectopic formation of mouse subcortical bone.

Finally, we examined whether WT SBD peptide enhance the ectopic bone formation induced by BMP2. The size, a μCT image, and total or trabecular bone mineral densities (BMD) of BMP2-induced ectopic bones were almost comparable in the presence and absence of WT SBD peptide (Figures. 6a, 6b and 6c). However, subcortical BMD was higher in the presence of 100 μg of WT SBD peptide than with BMP2 alone (Figure 6c). Fluorescence images of undecalcified sections revealed the bone formation activity of BMP2-induced ectopic bones. The calcein-labeled surface seemed to increase in BMP2 with 100 μg of WT SBD peptide compared with BMP2 alone (Figure 6d). Quantitative analysis indicated a significant increase in the mineralization surface in BMP2 with 100 μg of WT SBD peptide compared with BMP2 alone (Figure 6e). To clarify the inhibitory effects of WT SBD peptide on osteoclastic bone resorption, we stained bone marrows with HE and osteoclasts with TRAP. We observed similar numbers of TRAP-positive osteoclasts in ectopic bones in the presence and absence of WT SBD peptide (Figure 6f), suggesting that WT SBD peptide did not affect osteoclastic bone resorption. Meanwhile, WT SBD peptide at 200 μg did not enhance BMP2-induced cortical BMD gains (Figure 6).

Discussion

We previously demonstrated that BMP-induced NF-κB activation inhibited BMP-induced osteoblastogenesis at the level of Smad DNA binding via interaction between the TA2 domain of p65 and the MH1 domain of Smad4 (Hirata-Tsuchiya S et al., 2014). In the present study, we further identified the structural requirements for the direct association of the TA2 domain of p65 with the MH1 domain of Smad4. The peptide targeting p65-Smad4 interaction, which we named SBD peptide, disrupted both the interaction of TA2 with MH1 (as shown using purified recombinant protein) and the association of p65 with Smad4 (as shown by immunoprecipitation). These results led us to examine whether the peptide enhanced BMP-induced osteoblastogenesis *in vitro* and *in vivo*. WT SBD peptide stimulated differentiation and mineralization of osteoblastic cells in the presence of BMP2 but not in the absence of BMP2, suggesting that WT SBD peptide enhanced osteoblastogenesis in a BMP2-dependent manner. Furthermore, in p65-/- MEFs, WT SBD peptide failed to stimulate BMP2-induced ALP activity, due to the specificity of the SBD peptide. WT SBD peptide also increased subcortical BMD under our experimental conditions.

p65 contains at least two independent transcriptional activation domains (TADs) within its COOH-terminal 120 amino acids (Schmitz et al., 1994; Schmitz M.L. et al., 1995). Previous studies showed that the deletion of either TA1 or TA2 leaves a transcriptional activity, suggesting that the transcriptional activity of TADs on p65 is highly redundant (Schmitz et al., 1994; Schmitz M.L. et al., 1995). However, several stimuli, such as phorbol 12-myristate 13-acetate (PMA), increased the transcriptional activity of TA2 between amino acids 442 to 470, but not TA1. In this study, we found that MH1 of Smad 4 directly interacted with between amino acids 428-443 of TA2 domain of p65. Thus p65 might suppress Smad4 functions by stumuli-induced transcriptional activity of TA2 domain in p65.

NF-κB is functionally involved in immune and inflammatory responses, cell proliferation, tumorigenesis and preventing apoptosis (Jimi E. 2015; Ghosh S and Dass JF. 2016). In contrast to NF-κB, BMP signaling provides anti-proliferative differentiation signaling in osteoblasts and in other tissue. The BMP/Smad and NF-κB signaling systems seem to exert antagonistic effects. Previous work showed that NF-κB activity is high during bone development but decreases in adult bone (Krum SA et al., 2010). The inhibition of NF-κB enhanced osteoblast differentiation and bone formation *in vitro* and *in vivo*, restored the inhibitory effect of TNFα on BMP2-induced osteoblast differentiation and prevented bone loss in ovariectomized mice (Chang J et al., 2009; Yamazaki M et al., 2009; Alles M et al., 2010; Krum SA. et al., 2010; Hirata-Tsuchiya S et al., 2014). Although it is accepted that NF-κB is a negative regulator of osteoblast differentiation and bone formation, the molecular mechanism of the inhibitory effects is found to be various. The inhibition of NF-κB in differentiated osteoblasts of mice expressing a dominant-negative form of IKKβ under controlling *Bglap2* promoter showed increased BMD and bone volume due to the increased activity of osteoblasts by enhancing Fos-related antigen-1 (Fra1), an essential transcription factor involved in bone matrix formation *in vitro* and *in vivo* (Chang J et al., 2009). Whereas others have shown that the activated NF-κB antagonizes BMP/TGF-β signaling by enhancing Smad7 expression (Bitzer M et al., 2000). The activation of NF-κB suppressed osteogenesis of mesenchymal stem cells by targeting β-catenin via upregulation of microRNA-150-3p (Wang N et al., 2016). We have shown that p65 suppresses BMP signaling and BMP2-induced osteoblast differentiation by inhibiting DNA binding of Smad complex via direct interaction of p65 with Smad4 (Hirata-Tsuchiya S et al., 2014). Together, NF-κB might interfere the BMP signaling by inhibiting multiple steps.

The selective inhibitor for NF-κB enhances osteoblast differentiation and bone formation and is useful for bone regeneration (Chang J et al., 2009; Yamazaki M et al., 2009; Alles M et al., 2010; Krum SA. et al., 2010; Hirata-Tsuchiya S et al., 2014).

However, mice deficient in p65 die as embryos, suggesting that inhibition of the NF-κB pathway results in life-threatening side effects (Beg AA et al., 1995). Thus, the interacting domain of p65 with Smad4 might be a novel therapeutic target for treating diseases accompanied by bone loss without causing severe side effects. Based on these concepts, we identified the interaction domain between these two proteins and then generated SBD peptide, which inhibits the interaction. In fact, WT SBD peptide enhanced BMP2-induced osteoblast differentiation and mineralization *in vitro* without affecting proliferation in the presence or absence of BMP2. Moreover, neither SBD peptide affected TNFα-induced degradation of IκBα, phosphorylation of p65, or expression of IL-6, a target gene of NF-κB. These results strongly indicated that WT SBD peptides enhanced BMP2-induced osteoblast differentiation by prolonging the DNA binding activity of the Smad complex without affecting NF-κB signaling.

Although WT SBD peptide enhanced BMP2-induced osteoblastic differentiation in both MC3T3-E1 cells and primary osteoblasts, WT SBD peptide slightly enhanced BMP2-induced ectopic bone formation in particular, with increased subcortical BMD. We tested several concentrations (0, 20, 50, 100, 200, and 400 μg) of WT SBD peptide, and we observed enhancement at 100 μg of WT SBD peptide together with BMP2. As mentioned above, WT SBD peptide might suppress only one of multiple steps of the inhibitory effect of NF-κB signaling on BMP signaling. Because WT SBD peptide did not affect NF-κB signaling, which is also important for RANKL signaling (Jimi E and Ghosh S. 2013), the enhancement of trabecular bone by WT SBD peptide might have been remodeled by osteoclasts. Further experiments with different bone regeneration models are necessary to confirm the effect of WT SBD peptide on BMP-induced bone formation *in vivo*.

In conclusion, WT SBD peptide stimulated BMP2-induced osteoblast differentiation and bone formation in cortical bone. This augmentation of local bone formation could

be due to the acceleration of osteoblast differentiation by disruption of p65-Smad4 interaction with no effect on NF-κB signaling.

References

Alles, N., Soysa, N.S., Hayashi, J., Khan, M., Shimoda, A., Shimokawa, H., Ritzeler, O., Akiyoshi, K., Aoki. K., & Ohya. K. (2010). Suppression of NF-κB increases bone formation and ameliorates osteopenia in ovariectomized mice. *Endocrinology,* 151, 4626-4634.

Beg, A.A., Sha, W.C., Bronson, R.T., Ghosh, S., & Baltimore, D. (1995). Embryonic lethality and liver degeneration in mice lacking the RelA component of NF-κB. *Nature,* 376, 167-170.

Bitzer, M., von Gersdorff, G., Liang, D., Dominguez-Rosales, A., Beg, A.A., Rojkind, M., & Böttinger, E.P. (2000). A mechanism of suppression of TGF-β/SMAD signaling by NF-κB/RelA. *Genes and Development,* 14, 187-197.

Chang, J., Wang, Z., Tang, E., Fan, Z., McCauley, L., Franceschi, R., Guan, K, Krebsbach, P.H., & Wang, C.Y. (2009). Inhibition of osteoblastic bone formation by nuclear factor-κB. *Nature Medicine,* 15, 682-689.

Chen, J.S., & Sambrook, P.N. (2011). Antiresorptive therapies for osteoporosis: a clinical overview. *Nature Reviews Endocrinology,* 8, 81-91.

Ghosh, S., & Dass, J.F. (2016). Study of pathway cross-talk interactions with NF-κB leading to its activation via ubiquitination or phosphorylation: A brief review. *Gene,* 584, 97-109.

Hirata, S., Kitamura, C., Fukushima, H., Nakamichi, I., Abiko, Y., Terashita, M., & Jimi, E. (2010). Low-level laser irradiation enhances BMP-induced osteoblast differentiation by stimulating the BMP/Smad signaling pathway. *Journal of Cellular Biochemistry,* 111, 1445-1452.

Hirata-Tsuchiya, S., Fukushima, H., Katagiri, T., Ohte, S., Shin, M., Nagano, K., Aoki, K., Morotomi, T., Sugiyama, G., Nakatomi, C., Kokabu, S., Doi, T., Takeuchi, H., Ohya, K., Terashita, M., Hirata, M., Kitamura, C., & Jimi, E. (2014). Inhibition of BMP2-induced bone formation by the p65 subunit of NF-κB via an interaction with Smad4. *Molecular Endocrinology,* 28, 1460-1470.

Jimi, E., & Ghosh, S. Role of nuclear factor-κB in the immune system and bone. (2005). *Immunological Review,* 208:80-87.

Jimi, E. (2015). The Role of BMP Signaling and NF-κB Signaling on Osteoblastic Differentiation, Cancer Development, and Vascular Diseases--Is the Activation of NF-κB a Friend or Foe of BMP Function? *Vitamins and Hormones,* 99, 145-70.

Katagiri, T., & Watabe. T. (2016). Bone Morphogenetic Proteins. *Cold Spring Harbor Perspectives in Biology,* 8, 021899.

Katagiri, T., Yamaguchi, A., Komaki, M., Abe, E., Takahashi, N., Ikeda, T., Rosen, V., Wozney, J.M., Fujisawa-Sehara, A., & Suda, T. (1994). Bone morphogenetic protein-2 converts the differentiation pathway of C2C12 myoblasts into the osteoblast lineage. *Journal of Cell Biology,* 127, 1755-1766.

Kobayashi, Y., Uehara, S., Udagawa, N., & Takahashi, N. (2016). Regulation of bone metabolism by Wnt signals. *Journal of Biochemistry,* 159, 387-392.

Krum, S.A., Chang, J., Miranda-Carboni, G., & Wang, C.Y. Novel functions for NFκB: inhibition of bone formation. *Nature Reviews Rheumatology,* 6, 607-611.

Schmitz, M.L., dos Santos, Silva, M.A., Altmann, H., Czisch, M., Holak, T.A., & Baeuerle, P.A. (1994). Structural and functional analysis of the NF-κB p65 C terminus. An acidic and modular transactivation domain with the potential to adopt an alpha-helical conformation. *The Journal of Biological Chemistry,* 1994 269, 25613-25620.

Schmitz, M.L., dos Santos, Silva, M.A., & Baeuerle PA. (1995). Transactivation domain 2 (TA2) of p65 NF-κB. Similarity to TA1 and phorbol ester-stimulated activity and phosphorylation in intact cells. *The Journal of Biological Chemistry,* 270, 15576-15584.

Sugiyama, G., Takeuchi, H., Kanematsu, T., Gao, J., Matsuda, M., & Hirata, M. (2013). Phospholipase C-related but catalytically inactive protein, PRIP as a scaffolding protein for phospho-regulation. *Advances in Biological Regulation,* 53, 331-340.

Wang, N., Zhou, Z., Wu, T., Liu, W., Yin, P., Pan, C., & Yu, X. (2016). TNF-α-induced NF-κB activation upregulates microRNA-150-3p and inhibits osteogenesis of mesenchymal stem cells by targeting β-catenin. *Open Biology,* pii 150258.

Yamazaki, M., Fukushima, H., Shin, M., Katagiri, T., Doi, T., Takahashi, T., & Jimi, E. (2009). Tumor necrosis factor alpha represses bone morphogenetic protein (BMP)

signaling by interfering with the DNA binding of Smads through the activation of NF-κB. *The Journal of Biological Chemistry,* 284, 35987-35995.

Zhao, B., Katagiri, T., Toyoda, H., Takada, T., Yanai, T., Fukuda, T., Chung, U.I., Koike, T., Takaoka, K., & Kamijo, R. (2006). Heparin potentiates the in vivo ectopic bone formation induced by bone morphogenetic protein-2. *The Journal of Biological Chemistry,* 281, 23246-23253.

Zhao, B. (2017). TNF and Bone Remodeling. *Current Osteoporosis Reports,* 15, 126-134.

Figure Legends

Figure 1. Interaction between the NH_2-terminal region of the TA2 domain of p65 and the MH1 domain of Smad4. (a) GST and GST-TA2 were precipitated with glutathione-agarose, and His-MH1 was precipitated with nickel-nitrilotriacetic acid agarose beads. The proteins were then separated by SDS-PAGE (10%) and stained with Coomassie blue (left panel). Equal amount of GST and GST-TA2 were used in subsequent pull-down experiments. Recombinant His-MH1 was applied to GST-TA2 or GST alone immobilized on glutathione beads, followed by immunoblotting with anti-His antibody (right panel). Similar results were obtained in 3 independent experiments. (b) Schematic outlines of the truncation mutants of the TA2 domain of p65. RHD: Rel Homology Domain, TA: Transactivation Domain. (c) Recombinant His-MH1 was applied to GST-fusion truncation mutants of TA2 or GST alone immobilized on glutathione beads, followed by immunoblotting with the anti-His antibody. Similar results were obtained in 3 independent experiments.

Figure 2. Inhibition of p65-Smad4 interaction by cell-permeable peptide spanning the

p65 SBD. (a) GST pull-down analysis was done with either GST-TA2 or GST alone in conjunction with His-MH1 in the presence or absence of 100 μM of either WT SBD or Scr peptide. Similar results were obtained in 3 independent experiments. (b) COS7 cells were cotransfected with FLAG-tagged p65 and Myc-tagged Smad4 in the presence or absence of 10 μM of either WT SBD or Scr peptide for 24 hr. The whole-cell lysates were immunoprecipitated with anti-FLAG antibody and immunoblotted with an anti-Myc antibody. n.s.: non-specific bands. Similar results were obtained in 3 independent experiments.

Figure 3. SBD peptide enhanced BMP2-induced osteoblast differentiation. (a) MC3T3-E1 cells were treated with or without BMP2 (100 ng/ml) in the presence or absence of WT SBD (5 or 10 μM), Scr (10 μM) peptide or WT SBD without a poly-arginine (WT-polyR) for 72 hr. The cells were then fixed with an acetone-ethanol mixture and incubated with a substrate solution. ALP activity was then determined. Data are expressed as the mean ± SD (n=3). *, $p<0.01$, **, $p<0.05$. Similar results were obtained in 3 independent experiments. (b) Cells were stained for ALP activity. Similar results were obtained in 3 independent experiments. (c) p65-/- MEFs were treated with BMP2 (100 ng/ml) in the presence or absence of WT SBD (5 or 10 μM) peptide for 72 hr. ALP activity was then determined. Data are expressed as the mean ± SD (n=3). Similar results were obtained in 3 independent experiments. (d) MC3T3-E1 cells were transfected with either FLAG-tagged TA2 or FLAG-tagged TA2 (444-521) and then treated with BMP2 (100 ng/ml) for 72 hr. The cells were then fixed with an acetone-ethanol mixture and incubated with a substrate solution. ALP activity was then determined. Data are expressed as the mean ± SD (n=3). *, $p<0.05$. Similar results were obtained in 3 independent experiments. The total cell lysates were immunoblotted with with anti-FLAG antibody. Anti-β-actin was used as a loading control. Similar results were obtained in 3 independent experiments. (e) MC3T3-E1 cells were treated with or

without BMP2 (100 ng/ml) in the presence or absence of WT SBD (10 μM) or Scr (10 μM) peptide for 24, 48, and 72 hr. Total RNA was isolated, and type I collagen, osteonectin, or osteocalcin and GAPDH mRNA levels were analyzed using real-time PCR. Data are expressed as the mean ± SD (n=3). *, $p<0.05$, **, $p<0.01$. Similar results were obtained in 3 independent experiments. (f) Primary osteoblasts were treated with or without BMP2 (100 ng/ml) in the presence or absence of WT SBD (5 or 10 μM) or Scr (10 μM) peptide for 14 days. Cells were stained with alizarin red to determine mineralization. Scale bar corresponds to 100 μm. Alizarin red dye was extracted with 10% formic acid, and the absorbance at 405 nm was determined with a microplate reader. Data are expressed as the mean ± SD (n=3). *, $p<0.05$, **, $p<0.01$. Similar results were obtained in 3 independent experiments.

Figure 4. SBD peptide enhanced BMP-induced transcriptional activity of Smad1/5 without affecting NF-κB activity. (a) MC3T3-E1 cells were treated with or without BMP2 (100 ng/ml) in the presence or absence of WT SBD (10 μM) or Scr (10 μM) peptide for the indicated lengths of time. The total cell lysates were immunoblotted with anti-p-Smad1/5, Smad1 and Smad4 antibodies. Anti-β-actin was used as a loading control. Similar results were obtained in 3 independent experiments. (b) MC3T3-E1 cells were treated with or without BMP2 (100 ng/ml) in the presence or absence of WT SBD (10 μM) or Scr (10 μM) peptide for the indicated lengths of time. The chromatin from individual samples was precipitated using anti-p-Smad1/5 antibodies. The Id1 promoter was amplified by PCR from the precipitated DNA. Similar results were obtained in 3 independent experiments. (c, d) MC3T3-E1 cells treated with or without BMP2 (100 ng/ml) in the presence or absence of WT SBD (10 μM) or Scr (10 μM) peptide for 2 hr (c) or 24 hr (d). Total RNA was isolated, and Id1 (c), osterix (OSX) (d), and GAPDH mRNA levels were analyzed using real-time PCR. Data are expressed as the mean ± SD (n=3). *, $p<0.01$. Similar results were obtained in 3 independent

experiments. (e) MC3T3-E1 cells were treated with or without TNFα (10 ng/ml) in the presence or absence of WT SBD (10 μM) or Scr (10 μM) peptide for the indicated lengths of time. The total cell lysates were immunoblotted with anti-IκBα, anti-p-p65 and anti-p65 antibodies. Anti-β-actin was used as a loading control. Similar results were obtained in 3 independent experiments. (f) MC3T3-E1 cells were treated with or without TNFα (10 ng/ml) in the presence or absence of WT SBD (10 μM) or Scr (10 μM) peptide for 24 hr. Total RNA was isolated, and IL-6 and GAPDH mRNA levels were analyzed using real-time PCR. Data are expressed as the mean ± SD (n=3). *, $p<0.01$.

Figure 5. SBD peptide did not significantly affect BMP2-induced chondrogenesis during ectopic bone formation. One microgram of BMP2 was implanted subcutaneously to induce ectopic bone formation in the presence or absence of WT SBD peptide in mice (n=4). (a) After 1 week, the implants were removed and sections of the implants were stained with Alcian blue. Scale bar corresponds to 100 μm. The width of the column structure of cartilage (b) and the area of cartilage was divided by the area of the whole pellet (c) were measured. *, $p<0.05$.

Figure 6. SBD peptide stimulated BMP2-induced ectopic formation of mouse subcortical bone. One microgram of BMP2 was implanted subcutaneously to induce ectopic bone formation in the presence or absence of WT SBD peptide in mice (n=4). (a) After 3 weeks, the implants were removed and examined using soft X-ray analysis. Scale bar corresponds to 5 mm. (b) Micro-CT reconstruction images of ectopic bone in the presence or absence of WT SBD peptide in mice. Scale bar corresponds to 1 mm. (c) BMD of the ectopic bones in the presence or absence of WT SBD peptide were measured using dual-energy X-ray absorptiometry. *, $p<0.01$. (d) Fluorescence images of undecalcified sections of ectopic bone in the presence or absence of WT SBD peptide.

Scale bar corresponds to 50 μm. The green color shows calcein labeling. (e) The distance between labeled deposits of ectopic bone in the presence or absence of WT SBD peptide was measured. *, $p<0.05$. (f) At 3 weeks after implantation, sections of the implants were stained with HE (top panels) and TRAP (bottom panels). Scale bar corresponds to 50 μm.

Supplemental Fig. 1. SBD peptide did not affect cell proliferation in the presence or absence of BMP2. MC3T3-E1 cells were treated with (B) or without (A) BMP2 (100 ng/ml) in the presence or absence of WT SBD (10 μM) or Scr (10 μM) peptide for the indicated periods. Cell proliferation was assessed. Data are expressed as the mean ± SD (n=3). Similar results were obtained in 3 independent experiments.

Supplemental Fig. 2. SBD peptide enhanced BMP2-induced osteoblast differentiation. (A) Primary osteoblasts were treated with or without BMP2 (100 ng/ml) in the presence or absence of WT SBD (5 or 10 μM) or Scr (10 μM) peptide for 72 hr. The cells were then fixed with an acetone-ethanol mixture and incubated with a substrate solution. ALP activity was then determined. Data are expressed as the mean ± SD (n=3). *, $p<0.01$. Similar results were obtained in 3 independent experiments. (B) Cells were stained for ALP activity. Similar results were obtained in 3 independent experiments.

ACKNOWLEDGMENTS

M.U., S.K., M.T., G.S., H.T., and E.J. performed the experiments. U.M., K.A. and Y.T. performed the radiological assessments. M.U., C.N., Y.M., Y.A., M.M. and K.K. prepared the histological samples. M.U., S.H.-T., S.K., M.Z., M.M., and C.K. reviewed the intermediate draft. E.J. designed the study, performed the literature review, prepared the initial and final versions of the paper, and submitted the document.

This work was supported by grants-in-aid from Kyushu Dental University Internal

Grants (to E.J.) and from the Ministry of Education, Culture, Sports, Science and Technology of Japan (JP16K11456 to M.Z., JP26293406 to C.K., and JP17K11706 to S.H.-T.).

The authors have declared no conflicts of interest.

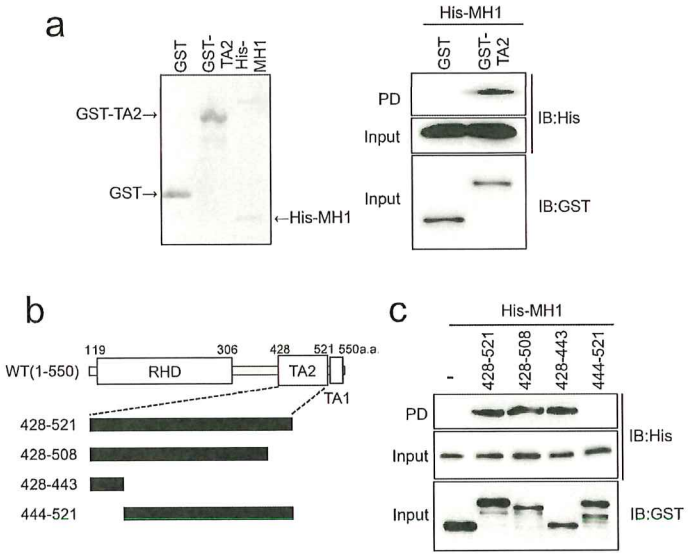

Figure 1

Figure 1. Interaction between the NH2-terminal region of the TA2 domain of p65 and the MH1 domain of Smad4.

254x338mm (300 x 300 DPI)

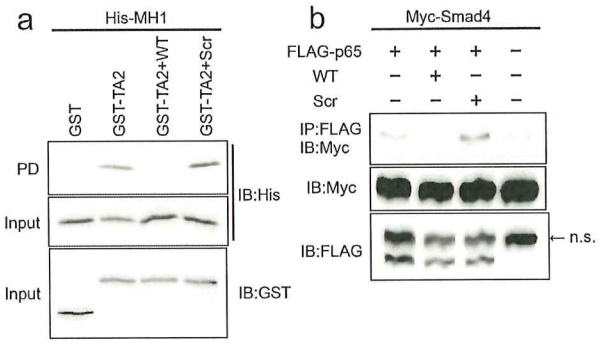

Figure 2

Figure 2. Inhibition of p65-Smad4 interaction by cell-permeable peptides spanning the p65 SBD.

254x338mm (300 x 300 DPI)

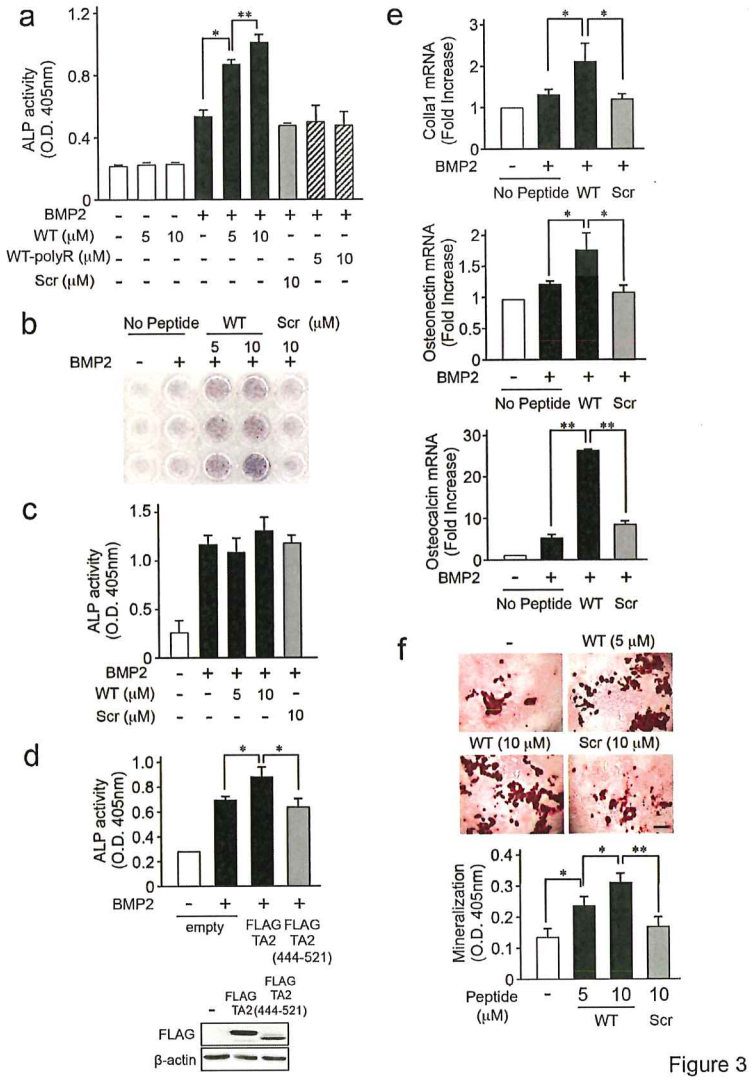

Figure 3

SBD peptide enhanced BMP2-induced osteoblast differentiation.

190x254mm (300 x 300 DPI)

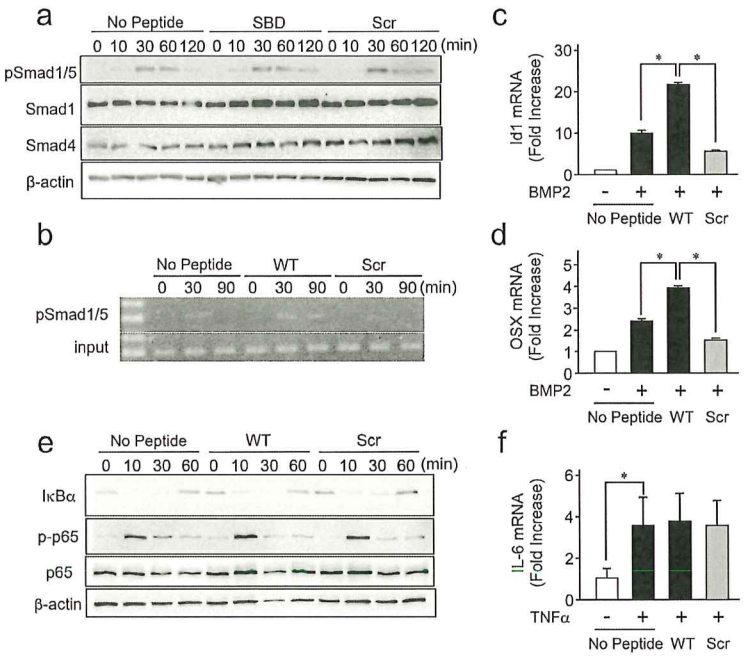

Figure 4

SBD peptide enhanced BMP-induced transcriptional activity of Smad1/5 without affecting NF-κB activity.

254x338mm (300 x 300 DPI)

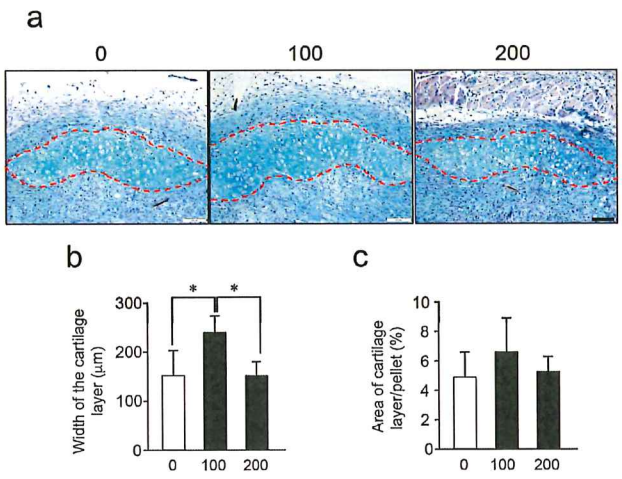

Figure 5

SBD peptide did not significantly affect BMP2-induced chondrogenesis during ectopic bone formation.

190x254mm (300 x 300 DPI)

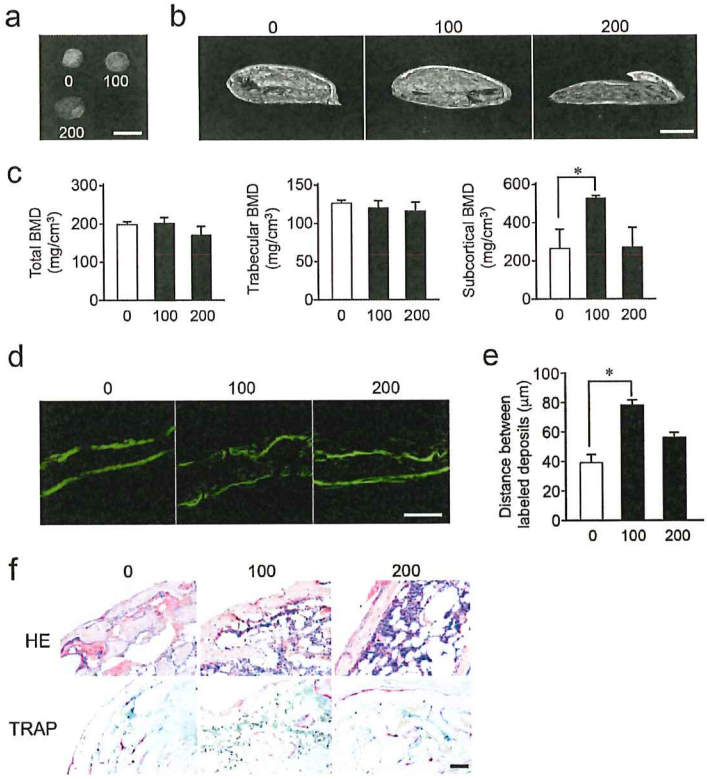

Figure 6

SBD peptide stimulated BMP2-induced ectopic formation of mouse subcortical bone.

190x254mm (300 x 300 DPI)